International Journal of Engineering Inventions
e-ISSN: 2278-7461, p-ISSN: 2319-6491
Volume 15, Issue 6 [June 2026] PP: 26-32

Mn^{2+} Introduced Single Crystals of Zn Cs_2 $(SO_4)_2 \cdot 6H_2O$: Spectroscopic and Local Structure Studies

Maroj Bharati [a], Vikram Singh [a], Ram Kripal [b]
[a] *Department of Physics, Nehru Gram Bharti (DU), Jamunipur, Prayagraj, India*
[b] *EPR Laboratory, Department of Physics, University of Allahabad, Prayagraj-211002, India*
***Corresponding Author**: Ram Kripal*

Abstract
The superposition model is used to evaluate the crystal field and zero field splitting parameters of the Mn^{2+} introduced Zn Cs2 (SO4)2.6H2O (ZCS) single crystals. The obtained parameters correspond well with those from EPR. The result of experiment that the Zn^{2+} site is replaced by the Mn^{2+} ion in ZCS is verified. The crystal's optical spectra are found utilizing crystal field analysis program and crystal field parameters obtained above. A fair matching is observed with the experimental band positions. Thus, the experimental observations are confirmed by the theoretical investigation.

Keywords: *Inorganic compounds, Electron paramagnetic resonance, Zero field splitting, Single crystal, Crystal fields, Superposition model.*

Date of Submission: 06-06-2026 Date of acceptance: 16-06-2026

I. Introduction

EPR studies of impurity ion introduced crystals provide information on the nature of the site into which the impurity ion enters the crystal and its symmetry [1-2]. EPR of Mn^{2+} impurity ion has been largely studied in various single crystals because of sensitivity of its fine structure (zero field) splitting to small structural distortions in the crystal [3-5].

The superposition model (SPM) is employed to model the crystal field (CF) and zero field splitting (ZFS) parameters for uses in various other studies [6–10]. SPM and the point-charge model [11, 12, 13] are widely used to find the crystal field (CF) parameters. SPM has been proposed for CF under certain assumptions [14]. Obtaining a static spherical polar coordinate system (R_L, θ_L, Φ_L) for each ligand from the host crystal's X-ray structural data is important for SPM analysis on the CF. Mismatches of ionic size, ionic charge and inter-ionic bonding are likely to give some local distortion when transition metal ions are introduced. Experimental spin-Hamiltonian parameters for Mn^{2+} and Fe^{3+} in CaO and MgO crystals have been critically analyzed [15] yielding the SPM parameters and showing that the CF for 3d ions satisfies the superposition principle. SPM intrinsic parameters based on reliable ligand distances have been evaluated for the alkali earth oxides, [16].

The general formula $A_2^+ B^{2+} (XO_4)_2$. $6H_2$ O crystals are known as Tutton salt single crystals with A being a monovalent cation, B being a divalent cation (usually a transition metal ion) and X being sulfur or selenium [17–18]. Tutton salt crystals are famous isostructural crystal family having the same monoclinic symmetry, the space group $P2_1/a$ and two formula units per unit cell Z = 2 [19]. Tutton salt crystals are very important crystals because they are used widely in UV filters [20].

Zinc cesium sulfate hexahydrate (ZCS) crystals are crystallized in the monoclinic crystal system and belong to the Tutton salt crystals family. Having high purity, suitable crystal sizes and small transparency in the UV region, they could be the potential candidates for optoelectronic devices [21].

EPR study of Mn^{2+} introduced ZCS has been taken up at 298 K and the spin-Hamiltonian parameters have been reported [22]. From angular variation studies, it is noted that magnetic $[Mn (H_2O)_6]^{2+}$ complexes are formed when the Mn^{2+} ion replaces the divalent sites of the Tutton salt lattice. The a*bc axis system, where a* is perpendicular to b and c, (crystal axes) is used to discuss the orientations. The angular study of the spectrum suggested the crystal field symmetry to be orthorhombic.

In this study, the ZFS parameters D and E are determined for the Mn^{2+} ion in ZCS at 298 K (room temperature, RT) using CF parameters from SPM and perturbation equations [23]. The purpose is to locate the position of Mn^{2+} ion and the distortion occurring in the ZCS crystal. The results for the Mn^{2+} ion at the substitutional Zn^{2+} site in ZCS crystal with local distortion yield good correspondence with the EPR experimental values. The study's other goal is to determine how well the SPM technique and CF theory apply to Mn^{2+} ions in ZCS crystals in order to create an SPM parameter database. This will evaluate molecular nanomagnet (MNM) design and computer simulation of their spectroscopic and magnetic properties. The transition ion-based MNM include single-molecule magnets (SMM) [24], single-chain magnets (SCM) [25], and single ion magnets (SIM) [26]. Due to interesting properties of MNM, like magnetization's macroscopic quantum tunneling and possible uses in high-density information storage and quantum computing, the above systems have attracted many scientists and researchers [23, 24]. We have various synthesized SCM or SMM systems with $Mn^{2+}$and Cr^{3+} ions [27]. Since model calculations for simpler crystal systems can be used as a basis for more complex ones, the parameters of the model in this study may be used for ZFS parameter computations for Mn^{2+} ions at appropriate sites in molecular nanomagnets. The present modeling process can be employed to get different crystals of scientific and industrial value in many other ion-host systems.

II. Crystal Structure

The crystal structure of Tutton salt ZCS is monoclinic with space group P 2_1/ a [28]. The unit cell's parameters are: Z = 2, β = 106.94°, a = 9.314, b = 12.817 and c = 6.369 Å. All other divalent cations in the unit cell are in general positions, with the two inequivalent ones located at points (0, 0, 0) and (1/2, 1/2, 0). Water molecules form a slightly warped octahedron around each divalent cation. The point symmetry group, which describes the site symmetry for Zn^{2+} ion, is D_{2h} [28]. Figure 1 shows the symmetry adopted axis system (SAAS) and ZCS crystal structure.

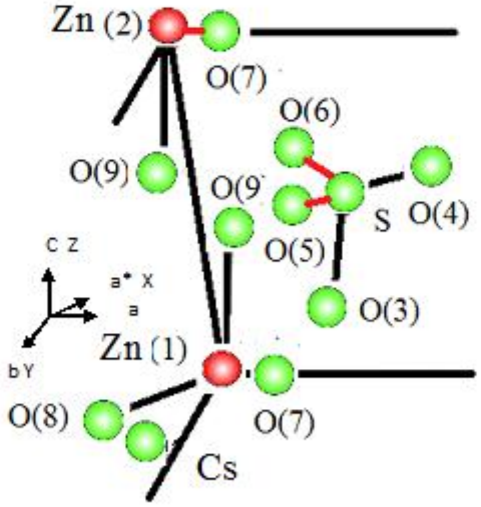

Fig. 1. The symmetry-adopted axis system (SAAS) and the room-temperature crystal structure of ZCS.

III. Crystal Field and Zero Field Splitting Parameter Calculations

The EPR spectra of Mn^{2+}: ZCS may be analyzed with the spin Hamiltonian [7]:

$$E(S_x^2 - S_y^2) + D\left\{S_Z^2 - \frac{1}{3}S(S+1)\right\} + \mu_B B.g.S = \mathscr{H} \qquad (1)$$

where B, μ_B, g, D and E are the applied magnetic field, Bohr magneton, splitting factor, second rank axial, and second rank rhombic ZFS parameters [29–30]. Fig. 1 shows the laboratory axes x, y, and z as well as the modified crystallographic axes a*, b, and c (a* is normal to axes b and c). The directions of metal-ligand bonds being mutually perpendicular are referred to as the symmetry adopted axes (SAA) or the local symmetry axes of the site. As shown in Fig.1, the axis-Z of SAAS is along the crystal axis- c, and (X, Y) are perpendicular to the axis-Z. When Mn^{2+} ions are introduced in ZCS crystal, they occupy Zn^{2+} (1) sites with some local distortion in the lattice [31].

The Mn^{2+} ion spin Hamiltonian is given as [32],

$$\mathscr{H}_{o} + \mathscr{H}_{so} + \mathscr{H}_{ss} + \mathscr{H}_{c} = \mathscr{H} \tag{2}$$

$$\mathscr{H}_{c} = \sum B_{kq} C_q^{(k)} \tag{3}$$

where B_{kq}, in Wybourne notation, represent the CF parameters and $C_q^{(k)}$, the spherical tensor operators. $B_{kq} \neq 0$ in the orthorhombic symmetry crystal field only for k = 2, 4; q = 0, 2, 4. Using SPM, the CF parameters B_{kq} in ZCS are calculated [32].

The symmetry of the local field about Mn^{2+} ions in ZCS crystal is orthorhombic (OR-type I) (D_{2h} point symmetry group) [7], where the ZFS parameters D and E are provided as follows [33]:

$$D = \left(\frac{3\varsigma^2}{70P^2D'} \right) [-B_{20}^2 - 21\varsigma B_{20} + 2B_{22}^2] + \left(\frac{\varsigma^2}{63P^2G} \right) [-5B_{40}^2 - 4B_{42}^2 + 14B_{44}^2] \tag{4}$$

$$E = \left(\frac{\sqrt{6}\varsigma^2}{70P^2D'} \right) [2B_{20} - 21\varsigma] B_{22} + \left(\frac{\varsigma^2}{63P^2G} \right) [3\sqrt{10}B_{40} + 2\sqrt{7}B_{44}] B_{42} \tag{5}$$

Here G = 10B+5C, D' = 17B+5C, P = 7B+7C. B and C present Racah parameters and ς, the spin-orbit coupling parameter. With N, the average covalency parameter, $B = N^4 B_0$, $C = N^4 C_0$, $\varsigma = N^2 \varsigma_0$, where ς_0 gives free ion spin-orbit coupling parameter and B_0 and C_0 provide Racah parameters for free ion [32, 34]. $\varsigma_0 = 336$ cm^{-1}, $B_0 = 960$ cm^{-1} and $C_0 = 3325$ cm^{-1} for free Mn^{2+} ion [7].

The parameter N is found from $N = \left(\sqrt{B/B_0} + \sqrt{C/C_0} \right)/2$ using Racah parameters (B = 850 cm^{-1}, C = 2970 cm^{-1}) estimated from optical study of Mn^{2+} ion in ZCS [35].

The CF parameters using SPM are calculated [14, 33], with co-ordination factor $K_{kq}(\theta_j, \varphi_j)$ and intrinsic parameter $\overline{A_k}(R_j)$, as

$$B_{kq} = \sum_j K_{kq}(\theta_j, \phi_j) \bar{A}_k(R_j) \tag{6}$$

$\overline{A_k}(R_j)$ is determined from

$$\overline{A_k}(R_0) \left(\frac{R_0}{R_j} \right)^{t_k} = \bar{A}_k (R_j) \tag{7}$$

where the ligand's distance from the d^n ion is denoted by R_j, $\overline{A_k}(R_0)$ is the intrinsic parameter, R_0 is the reference distance of the ligand from the metal ion and t_k gives power law exponent. For Mn^{2+}introduced crystals, $t_2 = 3$ and $t_4 = 7$ [33]. As the co-ordination around Mn^{2+} ion is octahedral, $\overline{A_4}$ is calculated from the relation [33]

$$\overline{A_4}(R_0) = \frac{3}{4} Dq \tag{8}$$

From optical study [35], $Dq = 790$ cm^{-1}. Therefore, $\overline{A_4}(R_0) = 592.5$ cm^{-1}. For $3d^5$ ions the ratio $\frac{\overline{A_2}}{\overline{A_4}}$ falls in the range 8 - 12 [32, 36-38]. With $\overline{A_2} = 10\,\overline{A_4}$, $\overline{A_2} = 5925$ cm^{-1}.

IV. Results and Discussion

Using the ligand configuration around Mn^{2+} ion shown in Fig. 1 and SPM, the CF parameters of the Mn^{2+} ion at the Zn^{2+}(1) sites in ZCS are evaluated. Table 1 gives atoms' coordinates in ZCS single crystal with bond length R (with and without distortion) and angles θ, φ for site I. The volume V, the distortion index D and the bond angle variation σ^2 are 727.24Å^3, 0.62 and 25.79 deg^2, respectively. The distortion index D and the bond angle variation σ^2 quantify the deviations in bond lengths and angles from an ideal octahedral geometry which were calculated by the methods described in [39, 40]. The ZFS and CF parameters using reference distance R_0 = 0.200 nm are presented in Table 2. Table 2 shows that R_0 = 0.200 nm being slightly less than the sum of radii of ions (0.223 nm) of Mn^{2+} = 0.083 nm and O^{2-} = 0.140 nm with no distortion give ZFS parameters at octahedral substitutional site I to be different from the EPR experimental values [22]. Experimental parameters of ZFS |D| and |E| (10^{-4} cm^{-1}) for site I from EPR are 265.7, 32.0, respectively. |E|/|D| is obtained as 0.120 being smaller than the standard value 0.33 [30]. |D| and |E| estimated theoretically without distortion are larger than the EPR experimental values. The value of |E|/|D| is also larger than the standard value 0.33 [30]. Hence, local distortion is introduced into calculation. Using above value of R_0 and local distortion, the ZFS parameter values for substitutional octahedral sites I are in good correspondence with the EPR experimental ones [22]. The parameters $t_2 = 3$ and $t_4 = 7$ with transformation S2 for standardization [30] are used to get |E|/|D| ratio near to 0.33 and calculated ZFS parameters very near to experimental values from EPR. CF and ZFS parameters for Mn^{2+} in other similar host crystals [41-43] are also given in Table 2 for comparison (Racah parameters in these crystals are given in Table 2). It is observed from Table 2 that the values of CF and ZFS parameters in the present crystal are similar to the values found by earlier workers [41-43].

Table 1. Atoms' coordinates, bond length R (with and without distortion) and angles θ, φ in ZCS (site I) single crystal.

Position of Mn^{2+}	Ligands	x	y (Å)	z	R(nm)	θ^0	φ^o
	Without distortion						
Site : Substitutional Zn(1) (0.0000, 0.0000, 0.0000)	O7	0.1607	0.1106	0.1606	0.20985 R_1	85.61 θ_1	85.59 φ_1
	O8	-0.1702	0.1083	0.0125	0.21259 R_2	89.66 θ_2	94.59 φ_2
	O9	-0.0027	-0.0645	0.2944	0.20560 R_3	81.76 θ_3	90.07 φ_3
	O7'	-0.1607	-0.1106	-0.1606	0.20985 R_4	94.39 θ_4	94.40 φ_4
	O8'	-0 .1607	0.3894	0.6606	0.69657 R_5	84.56 θ_5	91.33 φ_5
	O9'	0.1607	0.6106	0.3394	0.81409 R_6	87.61 θ_6	88.87 φ_6
	With distortion						
I	O7				0.31245	72.11	87.09
	O8				0.30259	69.66	96.59
	O9				0.31560	63.77	92.07
	O7'				0.31985	79.39	90.40
	O8'				0.83657	82.56	91.33
	O9'				0.89909	89.61	90.87

Table 2. The Mn^{2+} doped ZCS crystal's CF and ZFS parameters.

	Parameters of CF (cm^{-1})					Parameters of ZFS ($10^{-4}cm^{-1}$)		
Host	B_{20}	B_{22}	B_{40}	B_{42}	B_{44}	|D|	|E |	|E|/|D|
		Without distortion						
ZCS Site I	-20353.5	-25126.5	4722.913	5023.685	7458.51	4289.4	2198.8	0.512 P
		With distortion						
ZCS Site I	-5578.00	2970.134	16.89844	68.11449	2559.525	265.7	88.4	0.332 P
						Exp. 265.7	32.0	0.120
ZnF2	− 920	3730	21,180	− 1390	− 12,660	32.8	− 120	[41]
						Exp. 31.5	− 113.5	
Zn (l-asn)2	− 2464.76	− 1039.89	1364.28	1457.19	355.7	227	69	0.303 [42]

					Exp.	228	58	0.254
KHS								
Site I	− 1728.26	345.07	− 94.51	24.08	− 1415.09	59.4	08	0.134 [43]
					Exp.	59	32	0.542

P = Present study, ZnF_2= zinc fluoride: B = 911, C = 3273 cm^{-1}; Zn (l-asn)$_2$ = bis (l-asparaginato) zinc: B = 858, C = 2620 cm^{-1}; KHS = potassium hydrogen sulphate: B = 627, C = 2580 cm^{-1}; Exp. = experimental.

The CFA computer program [44] and B_{kq} parameters (with distortion) are employed to calculate the optical spectra of Mn^{2+} doped ZCS single crystals. By diagonalizing the total Hamiltonian, the Mn^{2+} ion's energy band positions are estimated.

Table 3 presents the energy band positions (experimental and calculated) for substitutional site I [35].

Table 3. Calculated and experimental Energy bands of single crystal of ZCS doped Mn^{2+}.

Transition from $^6A_{1g}(S)$ state	Band experimental (cm^{-1})	Band calculated (cm^{-1}) I
$^4T_{1g}(G)$	18436	23609, 23615, 23879, 23933, 24125, 24187
$^4T_{2g}(G)$	22815	24276, 24289, 24479, 24516, 24557, 24599
$^4E_g(G)$	24783	24833, 24862, 24866, 24874
$^4A_{1g}(G)$	24850	24884, 24896
$^4T_{2g}(D)$	28003	26758, 26811, 27154, 27223, 28839, 28841
$^4E_g(D)$	29870	29190, 29221, 29737, 29810
$^4T_{1g}(P)$	32435	31097, 31133, 35241, 35313, 35441, 35522
$^4A_{2g}(F)$		36509, 36851
$^4T_{1g}(F)$	41460	40826, 40892, 40901, 41089, 41168, 41325

It is noted from Table 3 that the experimental and calculated energy band positions match reasonably well. Therefore, the theoretical study confirms the EPR experimental result [22, 35] that Mn^{2+} ions enter the ZCS crystal at substitutional Zn^{2+}(1) octahedral site. The evaluated model parameters may be utilized in ZFS parameter calculations for Mn^{2+} ions at appropriate molecular nano magnet sites.

V. Conclusions

To find the splitting parameters of zero field, the superposition model and perturbation theory are employed for ZCS single crystals introduced with Mn^{2+} ions. The calculated ZFS parameters correspond well with the experimental values from EPR. The calculated positions of the optical energy bands correspond reasonably well with those found from the experiment. Hence, the experimental observation that Mn^{2+} ions replace Zn^{2+} (1) sites in ZCS is verified by the theoretical study. The determined model parameters in this investigation may be utilized for ZFS parameter evaluations for Mn^{2+} ions at appropriate sites in molecular nanomagnets. The above modeling process may be helpful in exploring various crystals of different scientific and industrial values.

Acknowledgement

The authors are grateful to the Head of Physics Department of Allahabad University, Allahabad for providing facilities of the department and to Prof. C. Rudowicz of Faculty of Chemistry, Adam Mickiewicz University, Poznan, Poland for CFA program.

Declarations

Ethical Approval:

There were no human or animal subjects in this study, and it wasn't conducted in any protected or private locations. Corresponding locations did not require any special permissions.

Competing interests:

The authors certify that none of the work presented in this paper could have been influenced by any known competing financial interests or personal relationships.

Authors' contributions:

Vikram Singh and Maroj Bharati prepared the figure, wrote the manuscript, and carried out the computations.
Ram Kripal: concept and oversight.
The manuscript has been reviewed by all authors.

Funding:

There is no funding received..

Availability of data and materials:

Upon request, the data will be made available.

References

[1]. J. Gtjens, M. Sjdin, V.L. Pecoraro, S. Un, J. Am. Chem. Soc. 129 (2007) 13825–13827.

[2]. O.D. Jayakumar, I.K. Gopalakrishnan, R.M. Kadam, A. Vinu, A. Asthana, A.K. Tyagi, J. Cryst. Growth 300 (2007) 358–363.

[3]. J. A. Weil, J. R. Bolton, Electron Paramagnetic Resonance: Elementary Theory and Practical Applications; 2nd ed., Wiley, New York, 2007.

[4]. S. P. Rathee, S. S. Hooda, EPR and superposition-model analysis of zero-field splitting parameters for Mn^{2+} doped in $ZnNbOF_5.6H_2O$ and $CoNbOF_5.6H_2O$ single crystals, Indian J. Phys. 99(1)(2025)145-148.

[5]. D. Halder, Y. Jana, D. Piwowarska, P. Gnutek, C. Rudowicz, Tailoring single-ion magnet properties of coordination polymer $C_{11}H_{18}DyN_3O_9$ (Dy-CP) using the radial effective charge model (RECM) and superposition model (SPM), Phys. Chem. Chem. Phys.26(2024) 19947-19959.

[6]. C. Rudowicz, P. Gnutek, M. Açıkg¨oz, Superposition model in electron magnetic resonance spectroscopy – a primer for experimentalists with illustrative applications and literature database, Appl. Spectrosc. Rev. 54 (2019) 673–718.

[7]. A. Abragam, B. Bleaney, Electron Paramagnetic Resonance of Transition Ion, Dover, New York, 1986.

[8]. J.R. Pilbrow, Transition-Ion Electron Paramagnetic Resonance, Clarendon Press, Oxford, 1990.

[9]. B. G. Wybourne, Spectroscopic Properties of Rare Earth, Wiley, New York, 1965.

[10]. J. Mulak, Z. Gajek, The Effective Crystal Field Potential, Elsevier, Amsterdam, 2000.

[11]. R. Boˇca, Zero-field splitting in metal complexes, Coord. Chem. Rev. 248 (2004) 757–815.

[12]. M. G. Brik, N. M. Avram (Eds.). Optical Properties of 3d-Ions in Crystals: Spectroscopy and Crystal Field Analysis. Heidelberg: Springer, (2013), Y. Y. Yeung: Chapter 3, pp. 95-121.

[13]. A. K. Yadav, U. M. Tripathi, and R. Kripal, Theoretical Calculation of Zero-Field Splitting Parameters for Mn^{2+} in Potassium Hydrogen Sulphate, Appl. Magn. Reson. 53 (2022) 941–947.

[14]. D. J. Newman and B. Ng, The superposition model of crystal fields, Rep. Prog. Phys. 52 (1989) 699-763.

[15]. D. J. Newman, E. Siegel, Superposition model analysis of Fe^{3+} and Mn^{2+} spin-Hamiltonian parameters, J. Phys. C: Solid State Phys. 9 (1976) 4285-4292.

[16]. Y. Y. Yeung, Local distortion and zero-field splittings of $3d^5$ ions in oxide crystals, J. Phys. C: Solid State Phys. 21 (1988)2453-2462.

[17]. F. Bosi, G. Belardi, P. Ballirano, Structural features in Tutton's salts$K_2[M^{2+}(H_2O)_6](SO_4)_2$, with$M^{2+}$ = Mg, Fe, Co, Ni, Cu, and Zn, Am. Mineral. 94(2009) 74–82.

[18]. M. Wildner, D. Marinova, D. Stoilova, Vibrational spectra of $Cs_2Cu(SO_4)_2{\cdot}6H_2O$ and $Cs_2Cu(SeO_4)_2{\cdot}nH_2O$(n=4, 6) with a crystal structure determination of the Tutton salt $Cs_2Cu(SeO_4)_2{\cdot}6H_2O$, J. Mol. Struct. 1106(2016) 440–51

[19]. H.T. Montgomery, E.C. Lingafelter, The crystal structure of Tutton's salts. II. Magnesium ammonium sulfate hexahydrate and nickel ammonium sulfate hexahydrate Acta Cryst. 17(1964) 1478–9

[20]. M. de Oliveira, S. Ghosh, T. S. Pacheco, G. J. Perpétuo, C. J. Franco, Growth and structural analysis of ammonium nickel cobalt sulfate hexahydrate crystals, Materials Research Express 4(2017) 105036

[21]. A. Abu El-Fadl, A. M. Nashaat, Growth, structural, and spectral characterizations of potassium and ammonium zinc sulfate hydrate single crystals, Appl. Phys. A123 (2017) 339(11 pages).

[22]. V. K. Jain, EPR of Mn^{2+} in Tutton Salts , Z. Naturforsch. 32 a(1977) 1364-1367.

[23]. W. L. Yu, M.G. Zhao, Spin-Hamiltonian parameters of ^6S state ions. Phys. Rev. B 37(1988) 9254-9267.

[24]. G. Aromí, E. K. Brechin, Synthesis of 3d metallic single-molecule magnets, Struct. Bonding 122 (2006) 1-67.

[25]. C. Coulon, H. Misayaka, R. Clérac, Single-Chain Magnets: Theoretical Approach and Experimental Systems, Struct. Bonding 122 (2006) 163-206.

[26]. M. Murrie, Cobalt(II) single-molecule magnets, Chem. Soc. Rev. 39 (2010) 1986-1995.

[27]. C. van Wüllen, Magnetic anisotropy through cooperativity in multinuclear transition metal complexes: theoretical investigation of an anisotropic exchange mechanism, Mol. Phys. 111 (2013) 2392–2397.

[28]. H. Euler, B. Barbier, A. Meents, A. Kirfel, Crystal structure of Tutton's salts, $Cs_2[M^{II}(H_2O)_6](SO_4)_2$, M^{II} = Mg, Mn, Fe, Co, Ni, Zn, Z. Kristallogr. NCS 218 (2003) 409–413

[29]. C. J. Radnell, J. R. Pilbrow, S. Subramanian, M. T. Rogers, Electron paramagnetic resonance of Fe^{3+} ions in $(NH_4)_2SbF_5$. J. Chem. Phys. 62(1975) 4948-4952.

[30]. C. Rudowicz, R. Bramley, On standardization of the spin Hamiltonian and the ligand field Hamiltonian for orthorhombic symmetry. J. Chem. Phys. 83(1985) 5192- 5197.

[31]. B. N. Figgis, M. A. Hitchman, Ligand Field Theory and its Applications; Wiley, New York, 2000.

[32]. T. H. Yeom, S. H. Choh, M. L. Du, M. S. Jang, EPR study of Fe^{3+} impurities in crystalline $BiVO_4$. Phys. Rev. B 53(1996) 3415-3421.

[33]. T. H. Yeom, S. H. Choh, M. L. Du, A theoretical investigation of the zero-field splitting parameters for an Mn^{2+} centre in a $BiVO_4$ single crystal. J. Phys.: Condens. Matter 5(1993) 2017-2024.

[34]. C. K. Jorgensen, Modern Aspects of Ligand Field Theory; North- Holland, Amsterdam, 1971, p.305.

[35]. K. Purandar, J. L. Rao, S. V. J. Lakshman, Optical Absorption Spectrum of Mn^{2+} in Zinc Cesium Sulphte Hexahydrate, Acta Phys. Slov. 34(1984)195-207.

[36]. D. J. Newman, B. Ng (Eds.), Crystal Field Handbook; Cambridge University Press, Cambridge, 2000.

[37]. A. Edgar, Electron paramagnetic resonance studies of divalent cobalt ions in some chloride salts. J. Phys. C: Solid State Phys. 9(1976) 4303-4314.

[38]. R. Kripal, M. G. Misra, A. K. Yadav, P. Gnutek, M. Açıkgöz, C. Rudowicz, Theoretical Analysis of Crystal field Parameters and Zero field Splitting Parameters for Mn^{2+} ions in Tetramethylammonium Tetrachlorozincate, Polyhedron, 235(2023)116341.

[39]. W. H. Baur, The Geometry of Polyhedral Distortions. Predictive Relationships for the Phosphate Group, Acta Cryst. B30 (1974)1195-1215.

[40]. K. Robinson, G. V. Gibbs, P. H. Ribbe, Quadratic Elongation: A Quantitative Measure of Distortion in Coordination Polyhedra, Science 172(1971)567-570.

[41]. W.L. Yu, M.G. Zhao, Determination of the MnF_2 and ZnF_2 crystal structure from the EPR and optical measurements of Mn^{2+}, J. Phys. C Solid State Phys. 18(1985) L1087–L1090.

[42]. S. Pandey, R. Kripal, Zero field splitting parameters of Mn^{2+} in Bis (L-asparaginato) Zn (II) at interstitial orthorhombic symmetry site, Spectrochim. Acta A91(2012) 290–294.

[43]. A. K. Yadav, U. M. Tripathi, R. Kripal, Theoretical Calculation of Zero-Field Splitting Parameters for Mn^{2+} in Potassium Hydrogen Sulphate, Appl Magn.Reson.53(2022)941-947.

[44]. Y. Y. Yeung, C. Rudowicz, Crystal Field Energy Levels and State Vectors for the $3d^N$ Ions at Orthorhombic or Higher Symmetry Sites. J. Comput. Phys. 109(1993) 150-152.